

Fig. S1 FT-IR spectra of PAA-modified Fe₃O₄ nanoclusters (a) and Fe₃O₄@PPy/Pd nanocomposites (b).

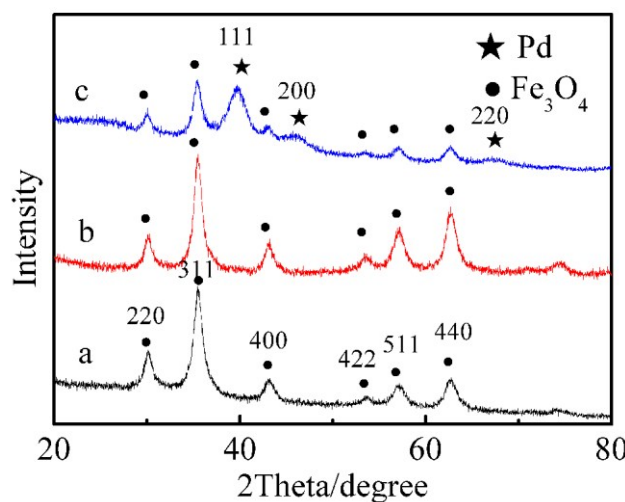


Fig. S2 XRD patterns of PAA-modified Fe₃O₄ nanoclusters (a) and Fe₃O₄@PPy/Pd nanocomposites synthesized in mixed solvent with the ethanol/water volume ratio at 1:1 (b) and pure water (c).

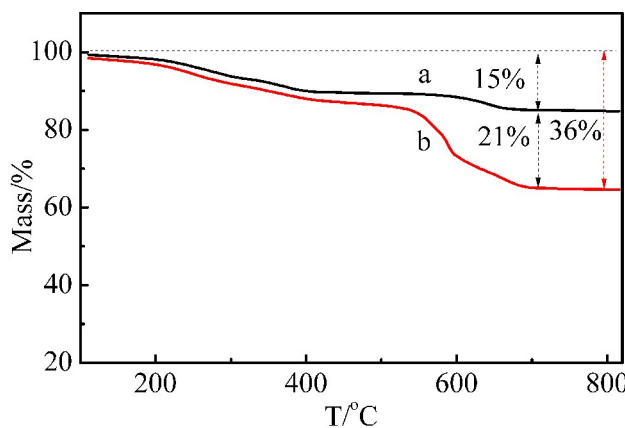


Fig. S3 TG curves of samples: PAA-modified Fe₃O₄ nanoclusters (a) and Fe₃O₄@PPy/Pd nanocomposites (b).

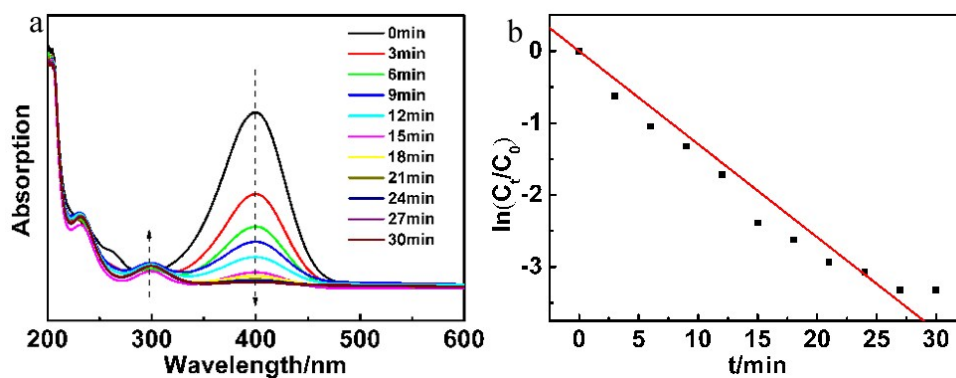


Fig. S4 Time-dependent UV/Vis spectra of 4-NP catalyzed by $\text{Fe}_3\text{O}_4@\text{PPy}/\text{Pd}$ nanocomposite (a), The plot of $\ln(C_t/C_0)$ against the reaction time (t) for the reduction of 4-NP (b).

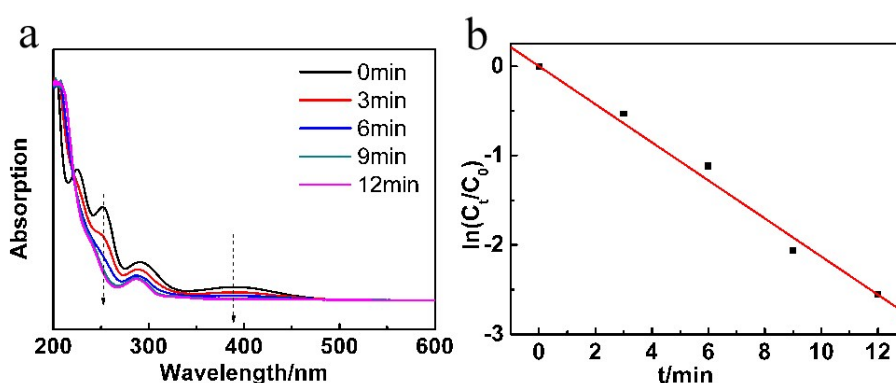


Fig. S5 Time-dependent UV/Vis spectra of 3-NP catalyzed by $\text{Fe}_3\text{O}_4@\text{PPy}/\text{Pd}$ nanocomposite (a), The plot of $\ln(C_t/C_0)$ against the reaction time (t) for the reduction of 3-NP (b).

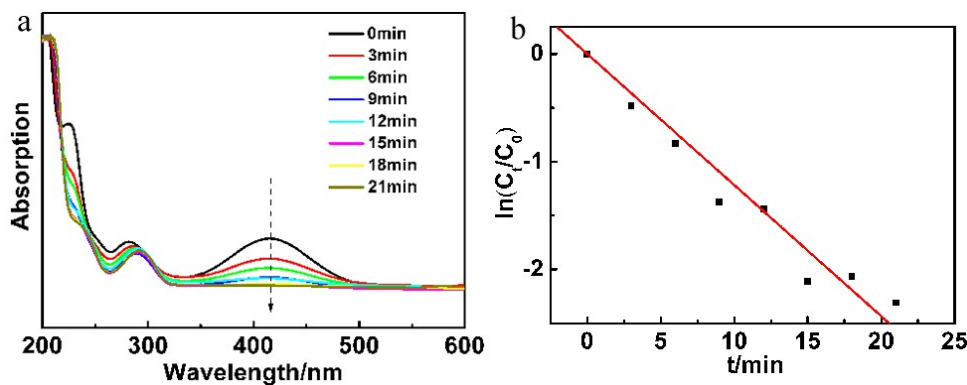


Fig. S6 Time-dependent UV/Vis spectra of 2-NP catalyzed by $\text{Fe}_3\text{O}_4@\text{PPy}/\text{Pd}$ nanocomposite (a), The plot of $\ln(C_t/C_0)$ against the reaction time (t) for the reduction of 2-NP (b).

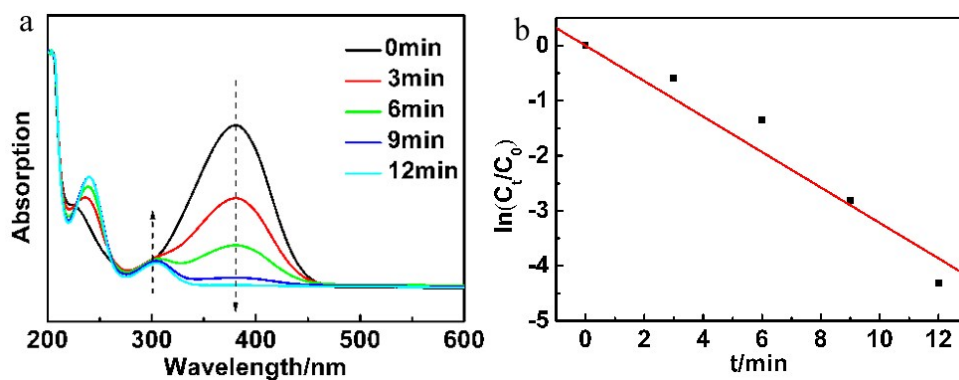


Fig. S7 Time-dependent UV/Vis spectra of 4-NA catalyzed by $\text{Fe}_3\text{O}_4@\text{PPy}/\text{Pd}$ nanocomposite (a), The plot of $\ln(C_t/C_0)$ against the reaction time (t) for the reduction of 4-NA (b).

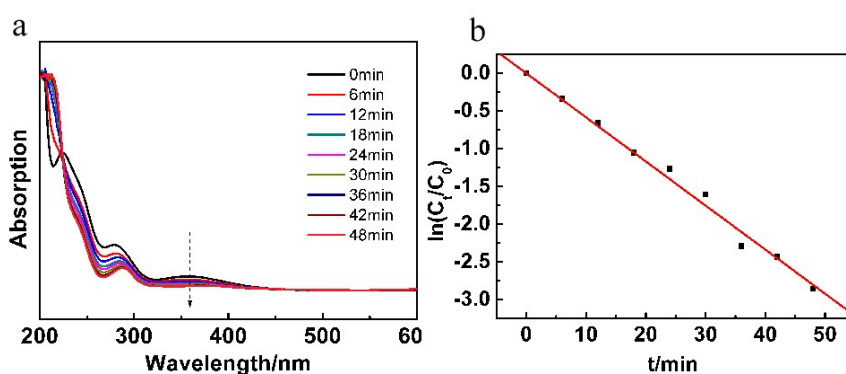


Fig. S8 Time-dependent UV/Vis spectra of 3-NA catalyzed by $\text{Fe}_3\text{O}_4@\text{PPy}/\text{Pd}$ nanocomposite (a), The plot of $\ln(C_t/C_0)$ against the reaction time (t) for the reduction of 3-NA (b).

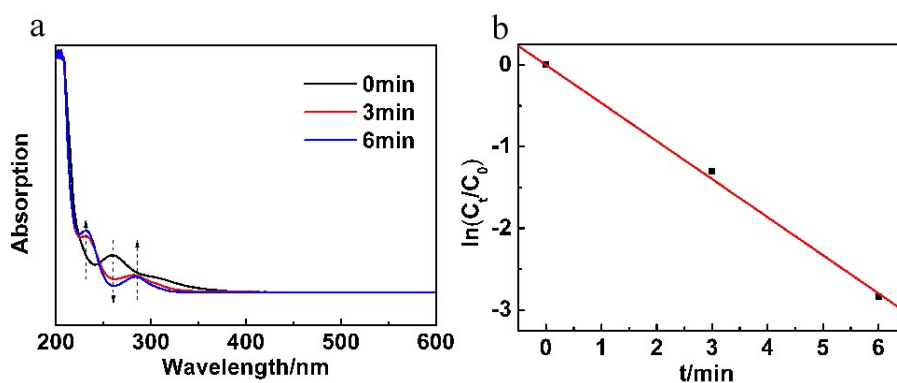


Fig. S9 Time-dependent UV/Vis spectra of 1-Chloro-2-nitrobenzene catalyzed by $\text{Fe}_3\text{O}_4@\text{PPy}/\text{Pd}$ nanocomposite (a), The plot of $\ln(C_t/C_0)$ against the reaction time (t) for the reduction of 1-Chloro-2-nitrobenzene (b).

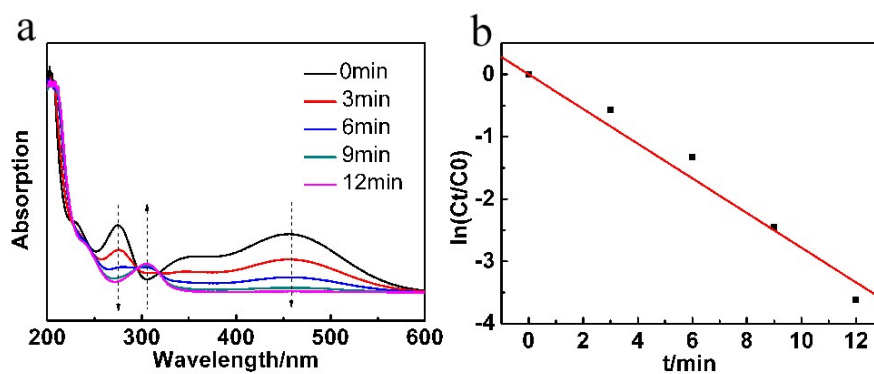


Fig. S10 Time-dependent UV/Vis spectra of 2-Amino-5-nitrophenol catalyzed by $\text{Fe}_3\text{O}_4@\text{PPy}/\text{Pd}$ nanocomposite (a), The plot of $\ln(C_t/C_0)$ against the reaction time (t) for the reduction of 2-Amino-5-nitrophenol (b).

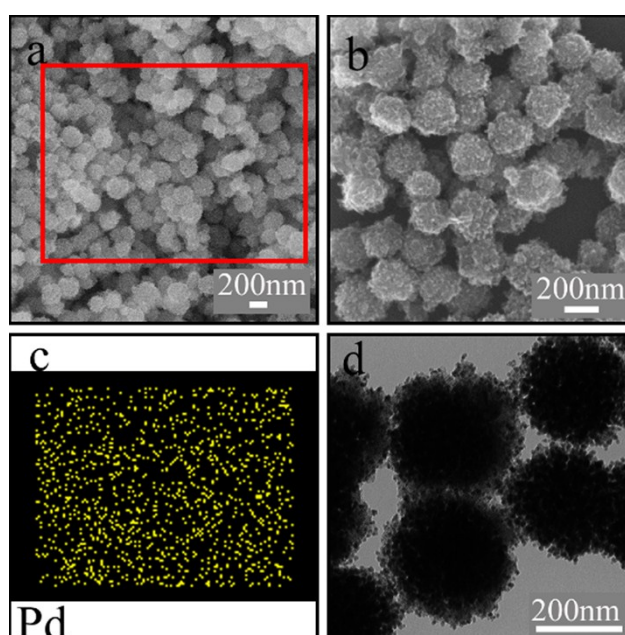


Fig. S11 SEM images (a, b), Pd element EDS mapping image (c) and TEM image (d) of the recovered $\text{Fe}_3\text{O}_4@\text{PPy}/\text{Pd}$ nanocomposites after ten cycles for catalytic reduction of 2-NA.

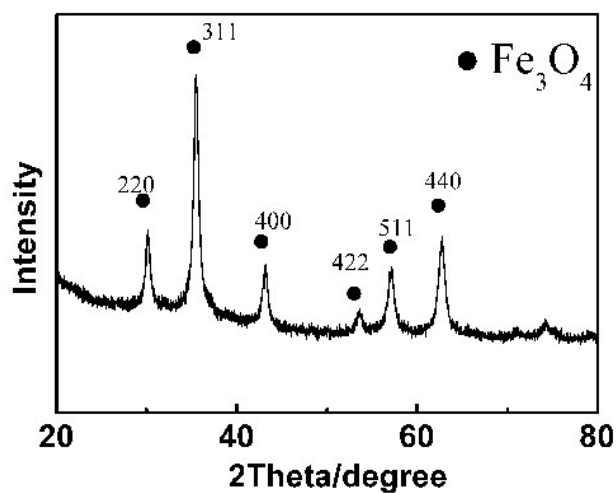


Fig. S12 XRD spectrum of the recovered $\text{Fe}_3\text{O}_4@\text{PPy}/\text{Pd}$ nanocomposites after ten cycles for catalytic reduction of 2-NA.

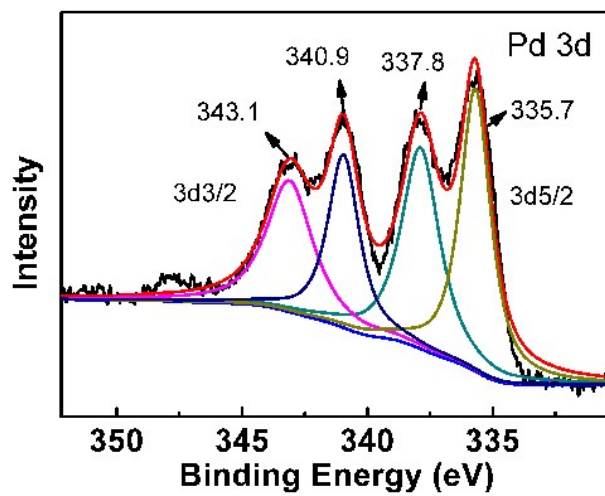


Fig. S13 XPS spectra of Pd 3d core electrons in the recovered $\text{Fe}_3\text{O}_4@\text{PPy}/\text{Pd}$ nanocomposites after ten cycles for catalytic reduction of 2-NA.